Journal of Alloys and Compounds 404–406 (2005) 150–154

Journal of ALLOYS AND COMPOUNDS

www.elsevier.com/locate/jallcom

Magnetic properties of Cr–CrH and YFe_2–YFe_2H_4

J.-C. Crivello, M. Gupta*

Thermodynamique et Physico-Chimie d'Hydrures et Oxydes,
E.A. 3547, Bât. 415, Science des matériaux, Université Paris-Sud, 91405 Orsay, France

Received 6 September 2004; accepted 14 September 2004

Abstract

Modifications of the electronic and magnetic properties of Cr and YFe_2 due to hydrogen absorption were studied using band structure calculations with the LMTO–ASA method.

For chromium, we show that the presence of hydrogen leads to a disappearance of antiferromagnetism. The paramagnetic state is the stable state of the hexagonal hydride CrH, in agreement with experimental results. We analyzed the role of the structural modifications and volume expansion of the Cr lattice and also the role of hydrogen on the electronic and magnetic properties. The increase of the density of states at the Fermi level from Cr to CrH is in agreement with measurements of heat capacity and magnetic susceptibility.

The stronger magnetization in ferromagnetic YFe_2H_4 compared to YFe_2 was explained by two antagonistic effects: (i) the lattice expansion due to hydrogen insertion which increases the magnetic moments M_S at the Fe sites, (ii) the metal-hydrogen interaction which slightly reduces M_S. In the hydride, the majority spin states of Fe are fully filled and the Fermi energy falls in a peak of the minority spin density of states. We found a small ferrimagnetic coupling of the 4d states of yttrium. Our results are in satisfactory agreement with experimental magnetic data.

Keywords: Electronic structure; Magnetic properties; Laves phase hydrides; Hydrogen storage materials

1. Introduction

Hydrogen absorption in metals and intermetallic compounds (IMC) is associated with a wide variety of alteration of their electronic, optic, conducting, superconducting and magnetic properties [1–3]. The role of hydrogen on the magnetic properties of IMCs is a very complex and fascinating topic that has been experimentally investigated since the pioneering work of Buschow et al. [4]. The insertion of hydrogen in a matrix is expected to affect the magnetic properties via several factors: magnetism is strongly dependent on interatomic distances that increase by the negative pressure effect associated with hydrogen uptake; in addition, the metal hydrogen bonding and the change in the Fermi level position are expected to strongly modify the magnetic interactions. To illustrate these effects, we have selected two examples, the disappearance of the antiferromagnetism of chromium Cr in hexagonal CrH [5–7], and the enhancement of ferromagnetism in YFe_2H_4 compared to the Laves phase intermetallic compound YFe_2 [8–10].

Using ab initio band structure calculations, investigation of electronic structures and magnetic characteristics of these compounds has been made in this paper. The role of hydrogen is analyzed in terms of modifications of crystallographic data and chemical bonding effects.

2. Computational method

The band structure calculations have been performed using the density functional theory in the local spin density approximation. The von Barth-Hedin [11] approach was used to determine the exchange and correlation term of the crystal potential. Since in the case of YFe_2H_4, we are dealing with unit cells containing a substantial number of atoms, we have used the self-consistent linear muffin–tin orbitals method within the atomic sphere approximation [12]. The so-called combined correction terms were included to account for the overlap of atomic spheres. For antiferromagnetic b.c.c. Cr, the

---

* Corresponding author. Tel.: +33 1 69 15 62 28; fax: +33 1 69 15 48 15.
E-mail address: michele.gupta@scmat.u-psud.fr (M. Gupta).

0925-8388/$ – see front matter © 2005 Elsevier B.V. All rights reserved.
doi:10.1016/j.jallcom.2004.09.080

spin-polarized calculations have been performed at 165 $\vec{k}$-points of the irreducible Brillouin zone (BZ), and with 270 $\vec{k}$-points for hexagonal CrH. We sampled the irreducible BZ with 95 and 140 $\vec{k}$-points, respectively for YFe_2 and YFe_2H_4. The densities of states (DOS) were calculated in a 1 mRy mesh with the linear energy tetrahedron method [13].

3. Results and discussion

3.1. Cr and hexagonal CrH

The insertion of hydrogen in b.c.c. chromium (with lattice parameter $a = 2.895$ Å) leads to a structural transition. In the present work we considered only the most experimentally investigated hexagonal anti-NiAs structure β-CrH phase with space group $P6_3mc$ [14] and lattice parameters $a = 2.72$ and $c = 4.42$ Å [5], although other cubic polymorphic phases have been reported [5]. While Cr has an antiferromagnetic behavior with a Néel temperature $T_N = 311$ K [15], it has been shown that the hydride CrH_x becomes paramagnetic for values of x larger than $x \approx 0.8$ with a strong Pauli susceptibility close to 5×10^{-6} emu/g [16].

The DOSs of the two spin directions of antiferromagnetic Cr are represented in Fig. 1. With a total width of ∼8 eV, the 3d bands of Cr, hybridized with s and p states, are characterized by two main structures associated to bonding and antibonding states separated by a valley characteristic of b.c.c. transition metals. The Fermi level E_F is located in this valley, thus the density of states at E_F is low, $N(E_F) = 0.61$ states/(eV-formula unit).The calculated magnetic moment, 0.60 μ_B per Cr atom, is in agreement with the experimental value of Bacon, 0.59 μ_B [15]. We find that the antiferromagnetic state is more stable than the paramagnetic state since its total energy is 5 mRy lower, it is thus the stable state.

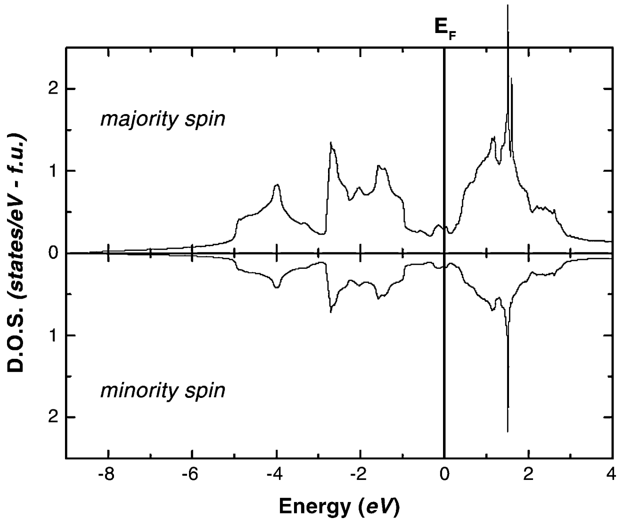

Fig. 1. Total density of states of the antiferromagnetic state of Cr for the two spin directions. The Fermi energy is chosen as origin.

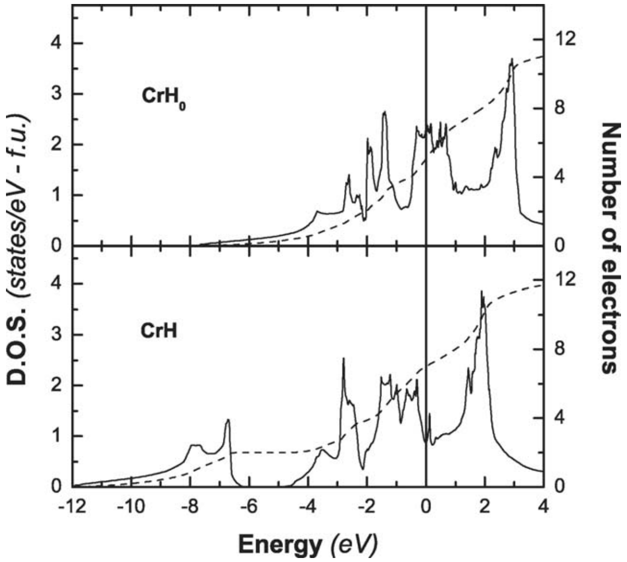

Fig. 2. Total density of states (full line, left hand side scale) and number of electrons (dashed line, right hand side scale) of: the Cr sublattice in hexagonal CrH without H atoms, "CrH_0", at the top, and the hexagonal hydride "CrH" at the bottom. The Fermi energy is chosen as origin.

In order to separate chemical from structural effects associated with the insertion of hydrogen, we present in the upper part of Fig. 2, the DOS of the so-called CrH_0 fictitious compound that corresponds to the h.c.p. Cr lattice of β-CrH where the hydrogen atoms have been removed. The DOS of CrH_0 is very different from that of b.c.c. Cr since the Cr–Cr distances increase by 7% and the coordination around Cr increases from 8 to 12. The DOS at E_F, $N(E_F) = 1.25$ states/(eV-formula unit) is much higher in CrH_0.

The total DOS of the hydride CrH is presented at the bottom of Fig. 2, for comparison with that of CrH_0, while the partial wave analysis of the DOS of CrH around the Cr and H sites is plotted in Fig. 3. A new structure appears between −12 and −6 eV below the Fermi level corresponding to the interaction of the s states of H with s, p and d states of Cr. This structure corresponds to one band thus to two electrons, it is separated from the conduction band by a gap of about 1.5 eV. From a comparison of the DOSs of CrH_0 and CrH, it is clear that the position of E_F shifts to higher energy in the hydride and $N(E_F)$ decreases substantially. For CrH, the calculated DOS at E_F, $N(E_F) = 0.88$ states/(eV-formula unit), is higher than its value $N(E_F) = 0.61$ states/(eV-formula unit) in Cr, in agreement with observed trends in the electronic specific heat coefficient that increases from 1.4 to 4.5 mJ/(g mol K) from Cr to CrH [17], magnetic susceptibility data [16], recent full-potential linear augmented plane-wave method calculations [7] and preliminary band structure results [18].

If we impose to CrH a polarization of spins on Cr with antiparallel ordering, we observe a quick cancellation of the moments during the self-consistent iterations and a convergence towards the paramagnetic state. The insertion of hydrogen thus leads to the destruction the antiferromagnetism of the Cr sublattice.

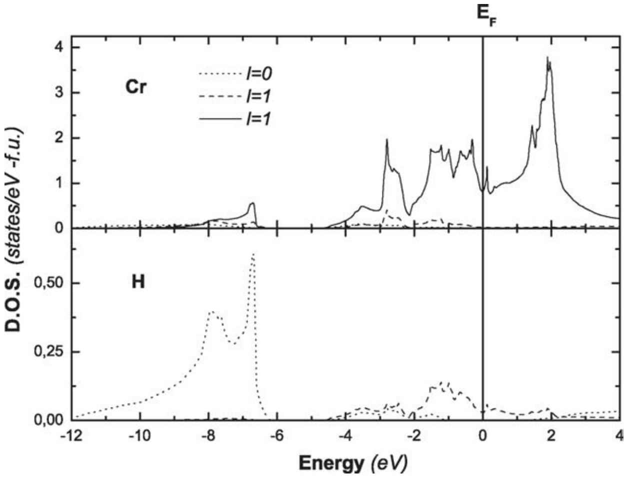

Fig. 3. Partial wave analysis of the DOS of hexagonal CrH around the atomic sites (d states: full line, p states: dashed line, s states: dotted line). The Fermi energy is chosen as origin.

3.2. YFe_2 and YFe_2H_4

The AB_2 Laves phase YFe_2 crystallizes in the cubic $MgCu_2$ type C15 structure with space group Fd-$3m$ (no. 227). Neutron diffraction data show that for $x = 3.3$ D/f.u. in YFe_2D_x, only the A_2B_2 tetrahedral sites (96 g) are occupied whereas for $x = 5$, there is some evidence for AB_3 site occupancy [8,9]. In our calculations on YFe_2H_4, we just considered the preferred A_2B_2 occupancy and we neglected the small rhombohedral distortion reported in YFe_2H_x for x greater than 3.3. The cubic lattice parameters 7.363 and 7.90 Å have been respectively used for YFe_2 and YFe_2H_4 [10,21].

The total DOS of ferromagnetic YFe_2 is plotted in Fig. 4 while its partial wave analysis around the different atomic sites are shown in Fig. 5 for each of the two spin directions. The calculated magnetic moment, $M_S = 2.86\,\mu_B$ is very close with several experimental data listed in Table 1. The magnetic moment is primarily localized on Fe, per iron atom it is smaller in the intermetallic compound than the value of 2.22 μ_B in b.c.c. iron. We find that the 4d orbitals of yttrium give a small negative contribution to the total magnetization, in agreement with calculations performed with different methods [19,20]. The exchange interaction leads to a decrease of the Y–Fe bonding between electrons of majority spin and in an increase of the interaction for the minority spin. In ferromagnetic YFe_2 the majority spin states are almost but not entirely filled, while the level Fermi falls in valley of the DOS of the 3d minority spin states. Thus, the total DOS at the Fermi energy $N(E_F) = 2.71$ states/(eV-formula unit) is rather low, the contributions from the minority and majority spin states are comparable.

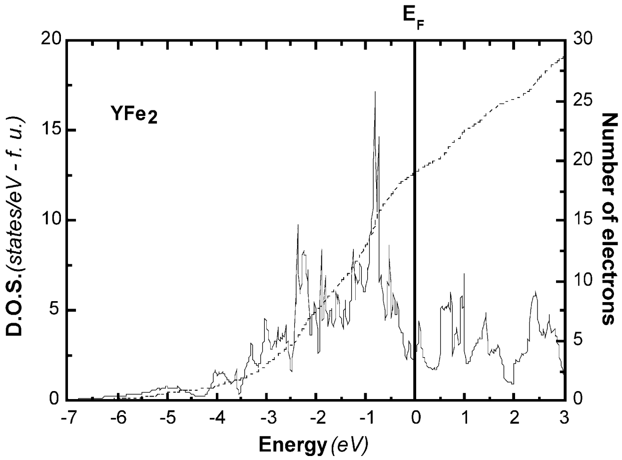

Fig. 4. Total density of states (full line, left hand side scale) and number of electrons (dashed line, right hand side scale) of ferromagnetic YFe_2. The Fermi energy is chosen as origin.

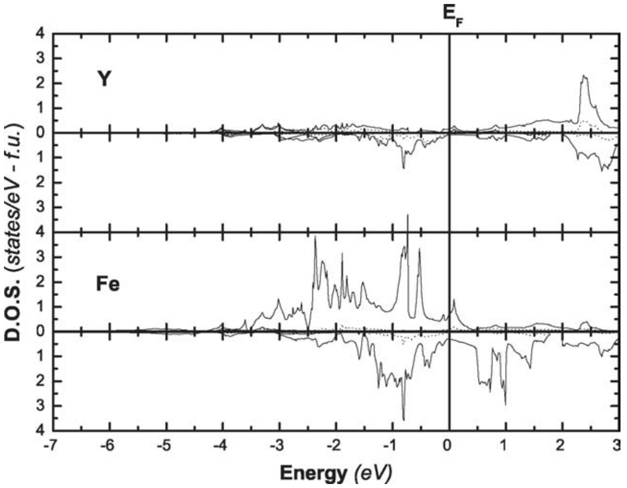

Fig. 5. Partial wave analysis of the DOS of YFe_2 for the two spin directions around the atomic sites (d states: full line, p states: dashed line, s states: dotted line). The Fermi energy is chosen as origin.

In order to separate lattice expansion effects and chemical effects due to the insertion of hydrogen, we present in Fig. 6 the results obtained for the ferromagnetic YFe_2H_0 fictitious compound obtained from YFe_2H_4 after removing the H atoms, the DOSs around the Y and Fe sites are plotted for each of the two spin directions in Fig. 6. A comparison of Figs. 5 and 6 indicate clearly that the 20% increase in the cell volume and the increased localization of the 3d orbitals, results in a decrease of the witdh of the iron d bands, and the exchange splitting is found to increase. YFe_2H_0 behaves like a strong ferromagnet, the majority spin d states are entirely filled while the Fermi level falls in a decreasing portion of a DOS peak below the valley of the minority spin d states. The DOS at E_F, 5.89 states/(eV-formula unit), increases from its

Table 1
Magnetic moments for YFe_2 and YFe_2H_4

YFe_2	YFe_2H_4
$M_S = 2.86\,\mu_B$ calculated	$M_S = 3.71\,\mu_B$ calculated
$M_S = 2.90\,\mu_B$ [4]	M_S ($YFe_2H_{\sim 4}$) = 3.66 μ_B [4]
	M_S (YFe_2H_x) = 3.80 μ_B [21]
	M_S ($YFe_2H_{4.2}$) = 3.62 μ_B [10]

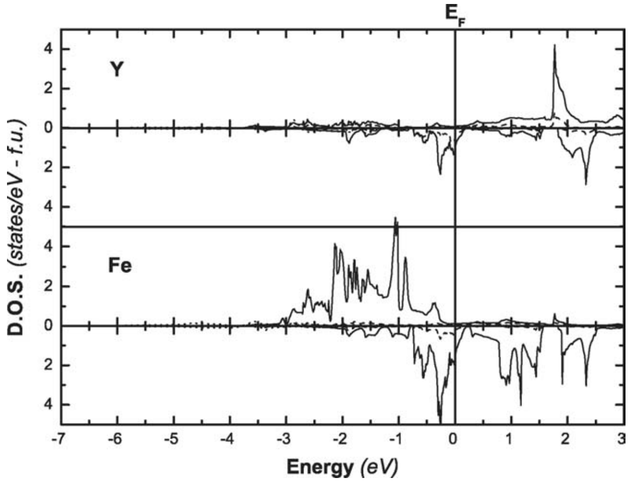

Fig. 6. Partial wave analysis of the DOS of the metal sublattice of YFe_2H_4 without H atoms, "YFe_2H_0", for the two spin directions around the atomic sites (d states: full line, p states: dashed line, s states: dotted line). The Fermi energy is chosen as origin.

value in YFe_2. At the Fe site, only the minority spin states strongly hybridized with the bonding Y 4d states, contribute significantly to $N(E_F)$, in contrast to the result obtained for YFe_2. The magnetic moment, 3.93 μ_B increases substantially from its value in YFe_2 due solely to the lattice expansion effect.

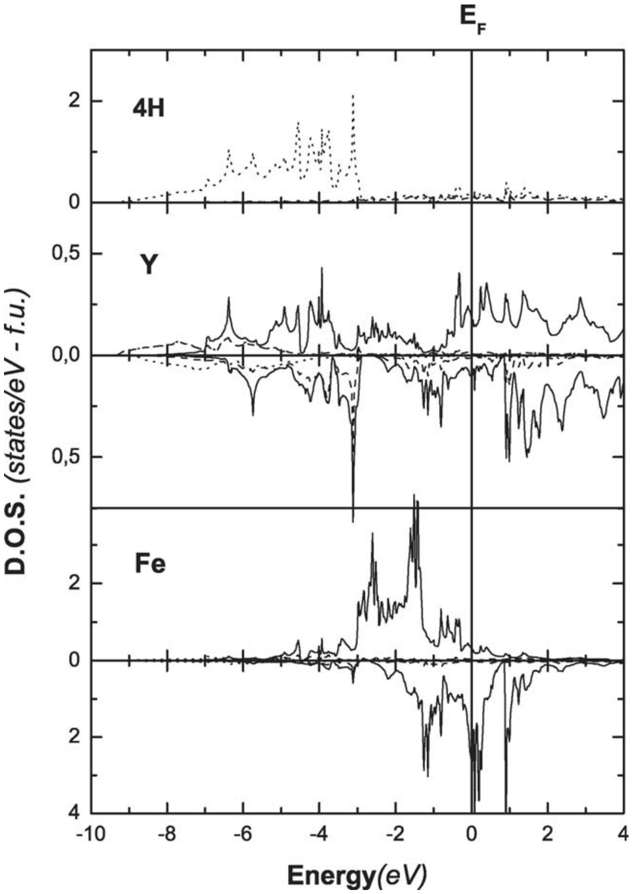

Fig. 7. Partial wave analysis of the DOS of YFe_2H_4 for the two spin directions around the atomic sites (d states: full line, p states: dashed line, s states: dotted line). The Fermi energy is chosen as origin.

The partial DOS analysis of ferromagnetic YFe_2H_4 is plotted in Fig. 7 around the different atomic sites. Metal-hydrogen interactions lead to a stabilization of the lowest portions of the Fe and Y bands and to the formation of a structure extending from −9 to −3 eV corresponding to four metal-hydrogen derived bands filled by eight electrons. The contribution to metal-hydrogen bonding is lightly more important per atom for iron than for yttrium. The calculated magnetic moment, $M_S = 3.71\,\mu_B$, is very close to the experimental values listed in Table 1. Comparing the values of M_S calculated for YFe_2, YFe_2H_0 and YFe_2H_4 we conclude that the lattice expansion effect leads to an important increase of M_S while the chemical effect due to the M–H interaction slightly reduces this value, in agreement with calculations performed by other methods or for different values of the H content [19,20]. In YFe_2H_4, E_F is located in a peak of 3d Fe minority states leading to a large value of the DOS at this energy, $N(E_F) = 6.52$ states/(eV-formula unit). A calculation of the total energy of the paramagnetic state of YFe_2H_4 has also been performed and was found 7.5 mRy higher than for the antiferromagnetic phase.

4. Conclusions

Using band structure calculations, we have studied the electronic and magnetic properties of Cr, YFe_2 and their hydrides CrH and YFe_2H_4.

For chromium, hydrogen loading leads to the destruction antiferromagnetism in hexagonal CrH. We analyzed the effect of structural modification and show that the shift of Fermi level due to the additional electron brought by hydrogen is responsible for the increase of the $N(E_F)$, in agreement with experimental observation.

We found that YFe_2 is more stable in the ferromagnetic phase than in the paramagnetic one. The magnetic moments, in agreement with the experimental results, are primarily localized on the iron atoms; a weak ferrimagnetic component associated to the more delocalized yttrium 4d states appears. A detailed study of the relative contributions of the lattice expansion and of the chemical effects associated to the metal-hydrogen bonding provides a clue to the origin of the increase in the magnetic moment of the ferromagnetic hydride YFe_2H_4. The calculated total magnetic moment is $3.71\,\mu_B$, in satisfactory agreement with the experimental values. This value results from two antagonistic effects: (i) the strong increase of M_S associated to the lattice expansion, (ii) the chemical effects due to the interaction of metal-hydrogen which tend to slightly decrease M_S.

Acknowledgements

We thank Institut de Développement et Recherche en Informatique Scientifique (IDRIS) of Centre national de la

Recherche Scientifique (CNRS) for providing the computing facilities for performing our electronic structure calculations. J-C C. thanks Institut National des Sciences et Techniques Nucléaires for providing four months financial support in 2001 during this research training work. M.G. thanks Drs. D.J. Singh and V. Paul-Boncour for fruitful discussions.

References

[1] L. Schlapbach, L. Schlapbach (Eds.), Topics in Applied Physics: Hydrogen in Intermetallic Compounds I, vol. 64, Springer-Verlag, 1988 and references therein.

[2] W.E. Wallace, in: G. Alefeld, J. Volk (Eds.), Topics in Applied Physics: Hydrogen in Metals I, vol. 28, Springer-Verlag, 1978, p. 9.

[3] K.H.J. Buschow, in: K.A. Gschneidner Jr., L. Eyring (Eds.), Handbook on the Physics and Chemistry of Rare Earths, vol. 6, North-Holland, Amsterdam, 1984, p. 1.

[4] K.H.J. Buschow, A.M. van Diepen, Solid State Commun. 19 (1976) 79;
K.H.J. Buschow, R.C. Sherwood, J. Appl. Phys. 48 (1977) 4643.

[5] B. Nowak, O.J. Żogał, K. Niedźwiedź, M. Tkacz, Z. Żołnierek, Physica B 193 (1994) 102.

[6] J.K. Poźniak-Fabrowska, B. Nowak, M. Tkacz, J. Alloys Compd. 322 (2001) 82.

[7] B. Nowak, J.K. Poźniak-Fabrowska, A. Szajek, J. Morkowski, M. Tkacz, J. Alloys Compd. 340 (2002) 67.

[8] M. Latroche, V. Paul-Boncour, A. Percheron-Guégan, F. Bourée-Vigneron, J. Solid State Chem. 133 (1997) 568.

[9] V. Paul-Boncour, S.M. Filipek, A. Percheron-Guégan, et al., J. Alloys Compd. 317–318 (2001) 83.

[10] V. Paul-Boncour, A. Percheron-Guégan, J. Alloys Compd. 293–295 (1999) 237.

[11] U. von-Barth, L. Hedin, J. Physica C 5 (1972) 1629.

[12] O.K. Andersen, Phys. Rev. B 12 (1975) 3600.

[13] G. Lehmann, M. Taut, Phys. Status Solidi (b) 54 (1972) 469.

[14] G. Albrecht, F.-D. Doenitz, K. Kleinstück, M. Betzl, Phys. Status Solidi 3 (1963) K249.

[15] G.E. Bacon, Neutron Diffraction, Clarendon Press, Oxford, 1968, p. 274.

[16] H.R. Khan, Ch.J. Raub, J. Less-Common Met. 49 (1976) 399.

[17] R. Viswanathan, H.R. Khan, A. Knödler, Ch.J. Raub, J. Appl. Phys. 46 (1975) 4088.

[18] A.C. Switendick, in: G. Alefeld, J. Völkl (Eds.), Topics in Applied Physics: Hydrogen in Metals I, vol. 28, Springer-Verlag, Berlin, 1978, p. 101.

[19] S.F. Matar, V. Paul-Boncour, Comptes Rendus de l'Académie des Sciences Série III, Chimie 3 (2000) 27;
V. Paul-Boncour, S.F. Matar, Phys. Rev. B 70 (2004) 184435.

[20] D.J. Singh, M. Gupta, Phys. Rev. B 69 (2004) 132403.

[21] K. Kanematsu, N. Ohkubo, K. Itoh, S. Ban, T. Miyajima, Y. Yamaguchi, J. Phys. Soc. Jpn. 65 (1996) 1072.